Simple control technique to eliminate source current ripple and torque ripple of switched reluctance motors for electric vehicle propulsion

Takayuki Kusumi, Takuto Hara, Kazuhiro Umetani, Eiji Hiraki
Graduate School of Natural Science and Technology
Okayama University
Okayama, Japan

Published in: IECON 2016 – 42nd Annual Conference of the IEEE Industrial Electronics Society pp.1876-1881

© 2016 IEEE. Personal use of this material is permitted. Permission from IEEE must be obtained for all other uses, in any current or future media, including reprinting/republishing this material for advertising or promotional purposes, creating new collective works, for resale or redistribution to servers or lists, or reuse of any copyrighted component of this work in other works.

DOI: 10.1109/IECON.2016.7793324

Simple Control Technique to Eliminate Source Current Ripple and Torque Ripple of Switched Reluctance Motors for Electric Vehicle Propulsion

Takayuki Kusumi, Takuto Hara, Kazuhiro Umetani, Eiji Hiraki
Graduate School of Natural Science and Technology
Okayama University
Okayama, Japan
p75s6ovi@s.okayama-u.ac.jp

***Abstract*— Switched reluctance motors (SRMs) are expected to be applied to propulsion systems of electric vehicles for their robust mechanical construction and cost-effectiveness. On the other hand, their large source current ripple and large torque ripple are main obstacles in practical applications of SRMs to vehicle propulsion. Certainly, a number of studies have been dedicated to address the torque ripple. However, unlike other motors driven by sinusoidal phase current waveforms, the large source current ripple of SRMs generally remains, even if the torque ripple is removed. The purpose of this paper is to propose a simple control technique of SRMs for vehicular propulsion by eliminating the source current ripple as well as the torque ripple. The proposed control is a current tracking control based on a pre-computed current profile. Because vehicular propulsion requires to instantaneously output large torque in sudden acceleration, SRMs tend to be designed to be propelled below the magnetic saturation in normal vehicle travel. Therefore, this proposed current profile is derived using a simple SRM analytical model without the magnetic saturation. In addition, the proposed current profile is determined so that the peak magnetic flux is minimized to offer high-speed current response at a high rotating velocity. Along with theoretical derivation of the proposed control, this paper also presents an experiment to verify the principle of the proposed control technique, which successfully revealed reduction of both the source current ripple and the torque ripple.**

Keywords—switrched reluctance motor; reluctance torque; source current ripple; torque ripple; current profile

I. INTRODUCTION

Recently, switched reluctance motors (SRMs) are expected to be applied to propulsion systems of electric vehicles for their robust mechanical construction and cost-effectiveness [1]. However, practical applications of SRMs to vehicular propulsion are hindered by their comparatively large source current ripple and torque ripple caused by mechanical and electrical nonlinearity [1][2].

As widely known, the large torque ripple is a severe problem because it can cause severe noise vibration, deteriorating the riding comfort. In addition, the large source current ripple can appear in the power supply to the inverter that drives the SRM. This source current ripple is also another severe problem because large AC current may flow from the main battery, thus deteriorating the battery lifespan. Certainly, an input smoothing capacitor that interfaces between the battery and the inverter is generally employed to decouple the source current ripple. However, the source current ripple generally contains large low frequency ripple generated by the cycle of the phase current except for the high frequency ripple generated by the switching. This low frequency source current ripple may not sufficiently decoupled by the input smoothing capacitor particularly at a low rotating velocity, because vehicular propulsion requires a wide variety of motor rotating velocity. Therefore, SRM drive for vehicular propulsion is intensely required to eliminate both the source current ripple and the torque ripple simultaneously.

Many studies have been dedicated to eliminating the torque ripple of SRM drive. There have been two major approaches for reducing the torque ripple: One is to optimize the magnetic design of the motor [3]–[7], and the other is to improve the control [8]–[27]. These prior techniques are proven to be effective for eliminating the torque ripple. However, it is worth noting that eliminating the torque ripple does not leads to eliminating the source current ripple in SRM drive unlike other motors driven by the sinusoidal phase current waveforms, such as the interior permanent magnet synchronous motors and the synchronous reluctance motors. Therefore, these prior techniques may still be insufficient for vehicular applications.

Besides, there also have been proposed techniques that address the source current ripple. For example, [28] proposed a novel control technique for a particular SRM drive circuit, which successfully verified elimination of the source current ripple. However, eliminating the source current ripple does not generally lead to eliminating the torque ripple. Therefore, this technique may also be insufficient for vehicular applications.

Certainly, some challenging studies addressed both the source current ripple and the torque ripple simultaneously. For example, [29][30] have proposed a novel comprehensive approach that combines both the control technique and the machine design. This technique can be applied to a pseudo-sinusoidal SRM, which has the inductance profile close to the sinusoidal waveform. Although this technique successfully eliminated the torque ripple with reduced source current ripple, this technique may have difficulty in application to many

commercially available SRMs, which do not have the sinusoidal inductance profile.

The purpose of this paper is to propose another novel control technique that can eliminate both the source current ripple and the torque ripple simultaneously. The proposed control does not depend on the machine design. Therefore, the proposed control is applicable to SRMs with arbitrary inductance profiles in general.

The proposed control is a current tracking control based on a pre-computed current profile. This current profile is derived using a simple SRM analytical model without the magnetic saturation. Certainly, SRMs are commonly driven with the magnetic saturation. However, SRMs for vehicular propulsion tend to be designed to be mainly driven below the magnetic saturation in the normal vehicle travel. The reason is that the vehicle propulsion generally requires a wide variety of torque output; and therefore, the magnetic flux linkage above the saturation level should be utilized to cover the instantaneous large torque output rather than the normal vehicle travel. Therefore, we neglect the magnetic saturation because we discuss elimination of the source current ripple and the torque ripple for the normal vehicle travel. In addition, the proposed current profile is determined so that the peak flux is minimized to improve the current response at a high rotating velocity.

The following discussion is composed of three sections. Section II presents the theoretical basis of the proposed control. Section III presents an experiment to verify the principle of the proposed control. Finally, section IV gives conclusions.

II. Proposed Control to Eliminate Source Current Ripple and Torque Ripple

The proposed control is a current tracking control based on a pre-computed current profile, similarly as in [29][30]. The current profile is amplified or attenuated to generate the current command value according to the torque command. Hence, the main issue is the method to determine this current profile. Below describes the theoretical basis of the method.

For convenience, we assume the three-phase concentrated-winding SRM as shown in Fig. 1. According to the aforementioned reason, we assume that the motor is driven below the magnetic saturation. Therefore, we neglect the magnetic saturation. As a result, we regard that the inductance of each phase winding is only dependent on the electrical angle. Furthermore, we approximate that the magnetic coupling between the phase windings is negligible in order to simplify our discussion. Then, the instantaneous torque τ is

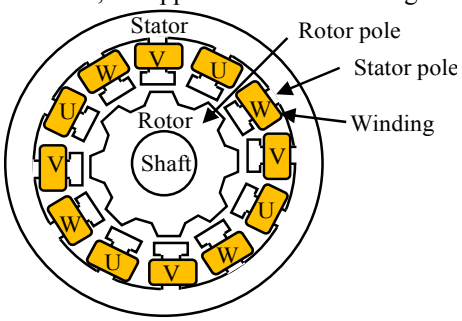

U, V, W: phases of the motor

Fig. 1. Sechematic illustraton of a three-phase concentrated-winding switched reluctance motor. (Sectional view)

$$\tau = \frac{1}{2}\frac{\partial L_U}{\partial \theta_M} i_U^2 + \frac{1}{2}\frac{\partial L_V}{\partial \theta_M} i_V^2 + \frac{1}{2}\frac{\partial L_W}{\partial \theta_M} i_W^2, \tag{1}$$

where L_U, L_V, and L_W are the inductance of phases U, V, and W, respectively; i_U, i_V, and i_W are the current of phases U, V, and W, respectively; and θ_M is the mechanical angle.

On the other hand, the source current can be obtained by dividing the sum of the instantaneous electric power provided to the phase windings by the voltage of the power supply to the inverter that drives the SRM. As is common in the SRM drive, we assume that the power supply has the constant voltage E. Noting that the voltage of phase U can be expressed as $\partial(L_U i_U)/\partial t$, we obtain the instantaneous electric power of phase U as $i_U \partial(L_U i_U)/\partial t$. Hence, the source current i_E is expressed as

$$\begin{aligned} i_E &= \frac{1}{E}\left(i_U \frac{\partial L_U i_U}{\partial t} + i_V \frac{\partial L_V i_V}{\partial t} + i_W \frac{\partial L_W i_W}{\partial t} \right) \\ &= \frac{\Omega}{E}\left(\frac{L_U}{2}\frac{\partial i_U^2}{\partial \theta_M} + i_U^2 \frac{\partial L_U}{\partial \theta_M} + \frac{L_V}{2}\frac{\partial i_V^2}{\partial \theta_M} + i_V^2 \frac{\partial L_V}{\partial \theta_M} \right. \\ &\quad \left. + \frac{L_W}{2}\frac{\partial i_W^2}{\partial \theta_M} + i_W^2 \frac{\partial L_W}{\partial \theta_M} \right), \end{aligned} \tag{2}$$

where Ω is the angler velocity of the rotor.

Because of the symmetry between the phases, we have $L_V(\theta_E)=L_U(\theta_E+4\pi/3)$ and $L_W(\theta_E)=L_U(\theta_E+2\pi/3)$, where θ_E is the electrical angle. Furthermore, we impose the same symmetry on the phase current, i.e. $i_V(\theta_E)=i_U(\theta_E+4\pi/3)$ and $i_W(\theta_E)=i_U(\theta_E+2\pi/3)$, as is natural in the motor drive. If we define θ_E using the number of the rotor poles P as $\theta_E=P\theta_M$, (1) and (2) can be rewritten as

$$\begin{aligned} \tau &= \frac{P}{2}\left\{ f(\theta_E) + f\left(\theta_E + \frac{2\pi}{3}\right) + f\left(\theta_E + \frac{4\pi}{3}\right) \right\}, \\ i_E &= \frac{P\Omega}{2E}\left\{ \frac{\partial}{\partial \theta_E} g(\theta_E) + f(\theta_E) + \frac{\partial}{\partial \theta_E} g\left(\theta_E + \frac{2\pi}{3}\right) \right. \\ &\quad \left. + f\left(\theta_E + \frac{2\pi}{3}\right) + \frac{\partial}{\partial \theta_E} g\left(\theta_E + \frac{4\pi}{3}\right) + f\left(\theta_E + \frac{4\pi}{3}\right) \right\}, \end{aligned} \tag{3}$$

where $f(\theta_E)$ and $g(\theta_E)$ are defined as

$$f(\theta_E) = \frac{\partial L_U(\theta_E)}{\partial \theta_E} i_U^2(\theta_E), \quad g(\theta_E) = L_U(\theta_E) i_U^2(\theta_E). \tag{4}$$

According to (3), we can see that the necessary and sufficient condition for constant τ regardless to θ_E (i.e. elimination of the torque ripple) is that $f(\theta_E)$ does not contain

the harmonics of multiples of three. However, we can also see that this does not necessarily lead to constant i_E (i.e. elimination of the source current ripple). Obviously, the necessary and sufficient condition for constant τ and i_E regardless to θ_E is that both $f(\theta_E)$ and $g(\theta_E)$ do not contain the harmonics of multiples of three.

This condition can be simplified by eliminating i_U from (4):

$$f(\theta_E)=\frac{\partial L_U(\theta_E)}{\partial \theta_E}\frac{g(\theta_E)}{L_U(\theta_E)}=\frac{\partial \ln L_U(\theta_E)}{\partial \theta_E}g(\theta_E). \tag{5}$$

(Note that $L_U(\theta_E)$ is always greater than 0.) Equation (5) shows that any pairs of $f(\theta_E)$ and $g(\theta_E)$ that satisfy (5) and do not contain the harmonics of multiples of three suffice to yield i_U that eliminate the source current ripple and the torque ripple simultaneously, as far as $g(\theta_E)$ remains positive regardless to θ_E. Then, the phase current i_U can be obtained according to

$$i_U(\theta_E)=\sqrt{g(\theta_E)/L_U(\theta_E)}. \tag{6}$$

Next, we discuss the method to determine pairs of $f(\theta_E)$ and $g(\theta_E)$ without the harmonics of multiples of three for the given inductance profile $L_U(\theta_E)$. For convenience, we set the origin of θ_E at the aligned position of phase U. Noting that $L_U(\theta_E)$ is an even function of θ_E, we approximate $\ln L_U(\theta_E)$ as

$$\begin{aligned}\frac{\partial \ln L_U(\theta_E)}{\partial \theta_E} &= K_1\sin\theta_E + K_2\sin 2\theta_E \\ &\quad + K_3\sin 3\theta_E + K_4\sin 4\theta_E + K_5\sin 5\theta_E.\end{aligned} \tag{7}$$

In addition, we assume that $g(\theta_E)$ has the following form, which does not contain the harmonics of multiples of three:

$$\begin{aligned}g(\theta_E) &= A_0 + A_1\sin\theta_E + A_2\sin 2\theta_E + A_4\sin 4\theta_E + A_5\sin 5\theta_E \\ &\quad + B_1\cos\theta_E + B_2\cos 2\theta_E + B_4\cos 4\theta_E + B_5\cos 5\theta_E.\end{aligned} \tag{8}$$

Then, we substitute (7) and (8) into (5) and determine the necessary conditions of A_0–A_5 and B_1–B_5 for eliminating the harmonics of multiples of three from $f(\theta_E)$. As a result, we have

$$A_4=-\frac{K_4-K_2+(K_1-K_5)\frac{K_5}{K_4}}{(K_1-K_5)\left(\frac{K_2}{K_4}-\frac{K_1K_5}{K_4^2}\right)+K_1-\frac{K_2K_5}{K_4}}A_1, \tag{9}$$

$$B_4=\frac{2K_3A_0+\left\{K_2+K_4-(K_1+K_5)\frac{K_5}{K_4}\right\}}{(K_1+K_5)\left(\frac{K_2}{K_4}-\frac{K_1K_5}{K_4^2}\right)+K_1-\frac{K_2K_5}{K_4}}B_1, \tag{10}$$

$$A_2=-\frac{K_5}{K_4}A_1-\left(\frac{K_2}{K_4}-\frac{K_1K_5}{K_4^2}\right)A_4, \tag{11}$$

$$B_2=-\frac{K_5}{K_4}B_1-\left(\frac{K_2}{K_4}-\frac{K_1K_5}{K_4^2}\right)B_4, \tag{12}$$

$$A_5=-\frac{K_5}{K_4}A_4,\quad B_5=-\frac{K_5}{K_4}B_4. \tag{13}$$

The necessary conditions (9)–(13) indicate that we can freely determine A_0, A_1, and B_1 as far as $g(\theta_E)$ remains positive regardless to θ_E, whereas the other parameters A_2, A_4, A_5, B_2, B_4, and B_5 are forced to satisfy (9)–(13). Therefore, various phase current profiles can eliminate both the source current ripple and the torque ripple simultaneously. Selection of the

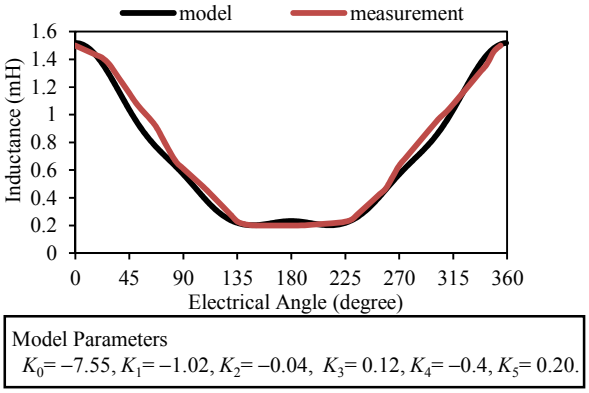

Fig. 2. Measured result and approximation model of the inductance profile of the experimental switched reluctance motor.

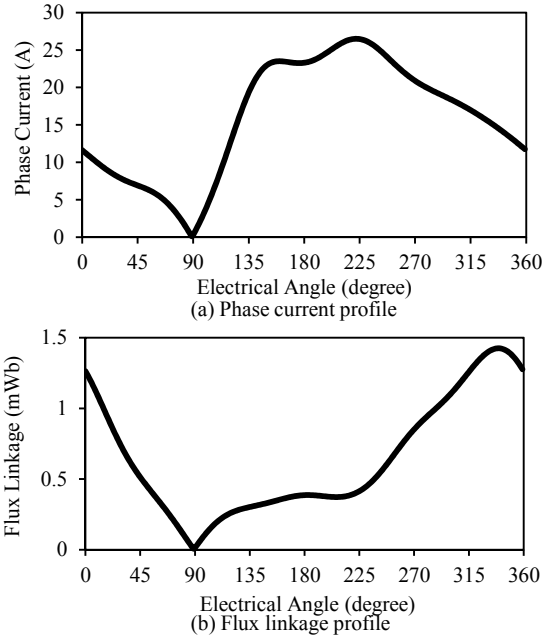

Fig. 3. An example of the phase current and flux linkage profiles of phase U in the proposed control.

profile depends on the design strategies adopted case by case.

In this study, we selected the profile so that the peak flux induction is minimized under the same torque output. This can improve the phase current response and enables this current profile to be applied to a high rotating velocity. For this purpose, we numerically searched by trial and error for parameters A_0, A_1, and B_1 that can minimize the peak flux.

For example, as for the SRM employed in the experiment presented in the next section, the inductance profile is measured as presented in Fig. 2. This inductance profile can be approximated according to (7) as shown in the same figure. As a result, the proposed current profile is calculated as shown in Fig. 3(a). In addition, the flux linkage profile is calculated as Fig. 3(b). Parameters A_1–A_5 and B_1–B_5 determined for this profile are presented in Table I.

Figure 4 presents the source current waveform and the torque waveform calculated based on (1) and (2) using the proposed current profile and the measured inductance profile. As expected in the theory, both of these waveforms are almost constant regardless to θ_E. Remaining ripples in the source current and the torque are caused by approximation error in the inductance profile modeling.

III. Experiment

Experiments were carried out to verify elimination of the source current ripple and the torque ripple by the proposed control. Figure 5 shows the SRM test bench employed for this experiment. In the test bench, a SRM and a hysteresis brake is mechanically coupled via an instantaneous torque meter. Table II shows the specifications of the test bench.

Figure 6 shows the schematic diagram of the inverter employed for driving the SRM in the experiment. Each phase are driven by a full-bridge circuit composed of two MOSFETs and two Schottky Barrier Diodes. The source current was measured between the two input smoothing capacitors.

Figure 7 shows the control diagram of the experimental motor test bench. The gate signals of the inverter are generated

TABLE I. Calculated Parameters for the Proposed Current Profile

A_0	3.63E-02	B_1	1.00E-02
A_1	-2.97E-02	B_2	5.14E-03
A_2	-1.11E-02	B_4	-1.00E-04
A_4	-2.73E-03	B_5	-5.00E-05
A_5	-1.37E-03		

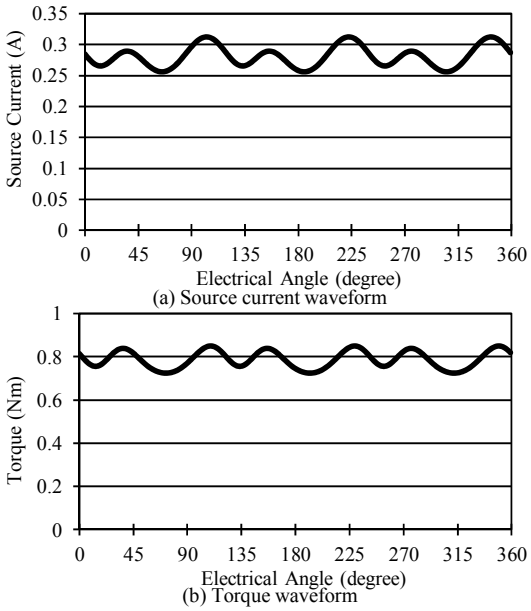

Fig. 4. Simulation results of the source current waveform and the torque waveform. (Rotation velocity: 75rpm, Power supply voltage: 20V.)

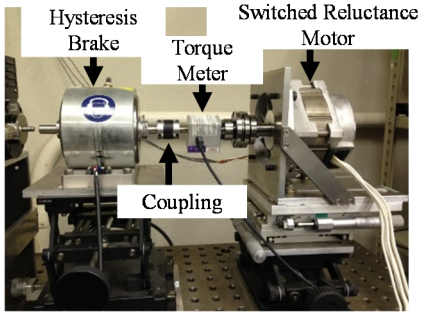

Fig. 5. Photograph of the experimental motor test bench.

TABLE II. Specifications of the Motor Test Bench

Instrument	Specifications
Motor	RB165SR-96VSRM (Motion System Tech. Inc.) 1.2kW, 96V, 6000rpm Stator: 12 poles, Rotor: 8 poles. Number of turns: 14T
Torque Meter	UTMII-5Nm (Unipulse Corp.)
Hysteresis Brake	AHB-6 (Magtrol Inc.)
Input Smoothing Capacitor	11.2mF, 5.6mF

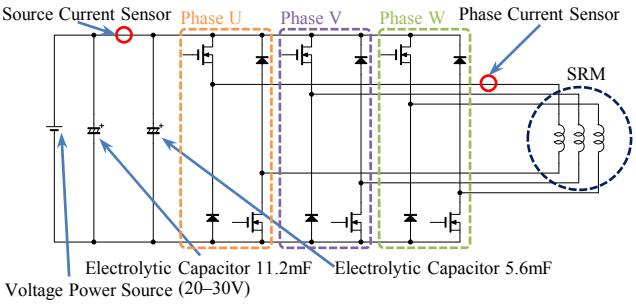

Fig. 6. Schematic diagram of the inverter employed to drive the switched reluctance motor in the test bench.

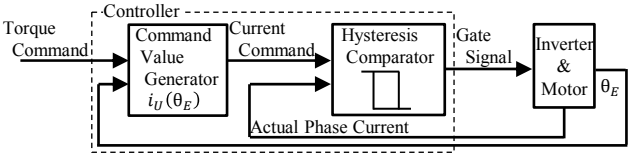

Fig. 7. Control diagram of the experimental motor test bench.

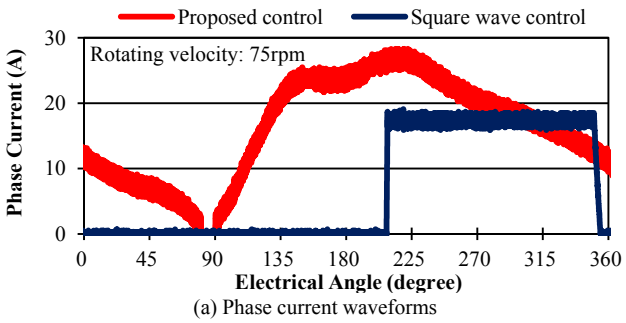

(a) Phase current waveforms

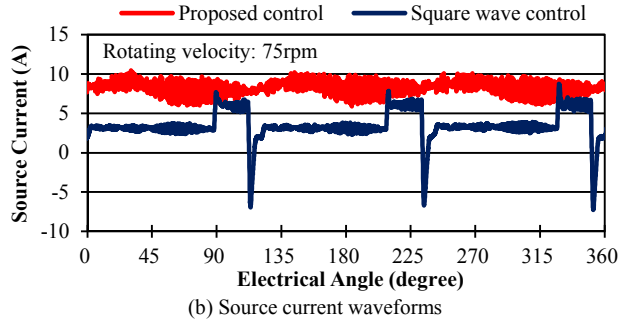

(b) Source current waveforms

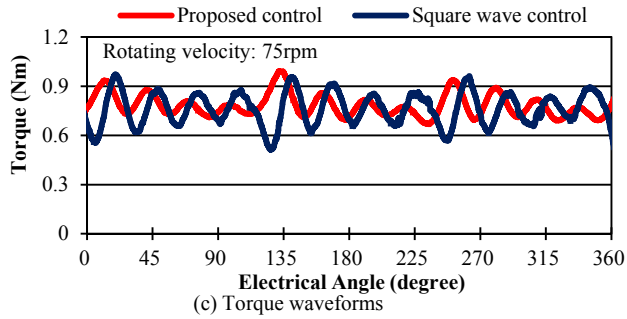

(c) Torque waveforms

Fig. 8. Experimental results of the torque and the source current at the rotating velocity of 75rpm.

by the hysteresis current tracking control. The hysteresis width is set at 1.5A.

The experimental SRM has the inductance profile presented in Fig. 2. Hence, the current waveform proportional to Fig. 3(a) is expected to eliminate the source current ripple and the torque ripple simultaneously. In this experiment, we drove the motor at the rotating velocity of 75rpm and 1500rpm using two different phase current waveforms: One is the proposed control and the other is the square wave control. The experimental current waveforms are shown in Fig. 8(a) and Fig. 9(a) at the rotating velocity of 75rpm and 1500rpm, respectively. The rising and falling angles of the phase current in the square wave control were set so that the torque ripple is minimized at the rotating velocity of 75rpm. As a result, the rising and falling angles of phase U were set at 208° and 352°, respectively.

Then, we compared the instantaneous torque waveform and the source current waveform between these two phase current waveforms under the same average torque. The average torque was 0.8N/m at 75rpm and 1.4N/m at 1500rpm.

The results of the instantaneous torque and the source current are presented in Fig. 8 and Fig. 9. We did not observe

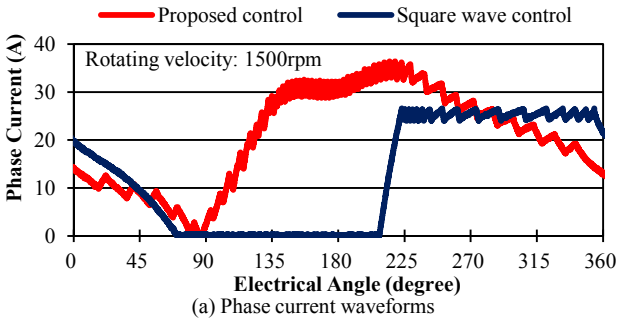

(a) Phase current waveforms

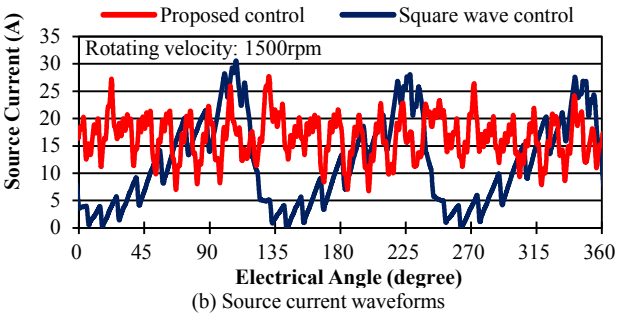

(b) Source current waveforms

Fig. 9. Experimental results of the source current at the rotating velocity of 1500rpm.

the instantaneous torque when the rotating velocity is 1500rpm, because the measurement results of the instantaneous torque meter contained significant parasitic mechanical resonance at 125Hz excited in the test bench.

As can be seen in Fig. 8(b) and Fig. 9(b), the source current ripple was successfully suppressed in the proposed control, whereas large ripple occurred in the square wave control. The source current ripples of the proposed control and the square wave control were within 9% and 101% of the average source current at 75rpm, respectively, and within 18% and 94% at 1500rpm, respectively. (This value was calculated based on the source current waveforms, after we eliminated the ripple directly caused by the hysteresis current tracking control.)

The source current waveforms of the square wave control contained large ripples. The positive and negative spikes found in the square wave control of Fig. 8(b) were caused by the rising and the falling of the phase current. These spikes covered the entire period in the square wave control of Fig. 9(b) because the rising and falling period of the phase current is long at a high rotating velocity.

In addition, as can be seen in Fig. 8(c), the torque ripple was also successfully suppressed in the proposed control as well as the square wave control. The torque ripple of the proposed control and the square wave control were within 19% and 33% of the average torque, respectively.

However, as can be seen in Fig. 8 and Fig. 9, the phase current of the proposed control was greater than that of the square wave control, although the average torque was almost the same between the two controls. In Fig. 8, the effective value of the phase current was 18Arms in the proposed control and 11Arms in the square wave control. In Fig. 9, the effective value was 23Arms in the proposed control and 17Arms in the square wave control. Therefore, the proposed control will lead

to reduction of the efficiency, although the proposed control can reduce the source current ripple and the torque ripple.

Consequently, we concluded that the experiment supported the proposed control.

IV. Conclusions

This paper presented a novel simple control technique for SRMs to eliminate the source current ripple as well as the torque ripple. The proposed control is the current tracking control with a pre-computed phase current profile, which can be systematically determined for SRMs with arbitrary inductance profiles. The experiment verified significant reduction of the source current ripple and the torque ripple.

Acknowledgment

This work was supported by JSPS KAKENHI Grant Number 15K18021.

References

[1] Z. Q. Zhu and C. C. Chan, "Electrical machine topologies and technologies for electric, hybrid, and fuel cell vehicles," in Proc. IEEE Vehicle Power Propulsion Conf., Harbin, China, pp. 1–6, Sept. 2008.

[2] W. Suppharangsan and J. Wang, "Experimental validation of a new switching technique for DC-link capacitor minimization in switched reluctance machine drives," in Proc. IEEE Int. Electric Machines Drives Conf., Chicago, USA, pp. 1031–1036, May 2013.

[3] S.-M. Jang, D.-J. You, Y.-H. Han, and J.-P. Lee, "Analytical design and dynamic characteristics of switched reluctance motor with minimum torque ripple," in Proc. Intl. Conf. Elect. Mach. Syst. (ICEMS2007), Seoul, South Korea, pp. 1236-1239, Oct. 2007.

[4] T. Higuchi, K. Suenaga, and T. Abe, "Torque ripple reduction of novel segment type switched reluctance motor by increasing phase number," in Proc. Intl. Conf. Elect. Mach. Syst. (ICEMS2009), Tokyo, Japan, pp. 1-4, Nov. 2009.

[5] A. Siadatan, M Asgar, V. Najmi, and E. Afjei, "A novel method for torque ripple reduction in 6/4 two rotor stack switched reluctance motor," in Proc. European Conf. Power Electron. Appl. (EPE2011), Birmingham, UK, pp. 1-10, Aug. 2011.

[6] M. A. Tavakkoli and M. Moallem, "Torque ripple mitigation of double stator switched reluctance motor (DSSRM) using a novel rotor shape optimization," in Proc. IEEE Energy Conversion Congr. Expo., Raleigh, NC, USA, pp. 848-852, Sept. 2012.

[7] Y. Li and D. C. Aliprantis, "Optimum stator tooth shapes for torque ripple reduction in switched reluctance motors," in Proc. IEEE Elect. Mach. Drives Conf., Chicago, IL, USA, pp. 1037-1044, May 2013.

[8] I. Husain and M. Ehsani, "Torque ripple minimization in switched reluctance motor drives by PWM current control," IEEE Trans. Power Electron., vol. 11, no. 1, pp. 83-88, Jan. 1996.

[9] A. M. Stankovic, G. Tadmor, Z. J. Coric, and I. Agirman, "On torque ripple reduction in current-fed switched reluctance motors," IEEE Trans. Ind. Electron., vol. 46, no. 1, pp. 177-183, Feb. 1999.

[10] L. Venkatesha and V. Ramanarayanan, "A comparative study of pre-computed current methods for torque ripple minimization in switched reluctance motor," in Proc. IEEE Ind. Appl. Conf., Rome, Italy, vol. 1, pp. 119-125, Oct. 2000.

[11] I. Agirman, A. M. Stankovic, G. Tadmor, and H. Lev-Ari, "Adaptive torque-ripple minimization in switched reluctance motors," IEEE Trans. Ind. Electron., vol. 48, no. 3, pp. 664-672, Jun. 2001.

[12] P. L. Chapman and S. D. Sudhoff, "Design and precise realization of optimized current waveforms for an 8/6 switched reluctance motor drive," IEEE Trans. Power Electron., vol. 27, no. 1, pp. 76-83, Jan. 2002.

[13] L. O. de Araujo Porto Henriques, P. J. Costa Branco, L. G. B. Rolim, and W. I. Suemitsu, "Proposition of an offline learning current modulation for torque-ripple reduction in switched reluctance motors: design and experimental evaluation," IEEE Trans. Ind. Electron., vol. 49, no. 3, pp. 665-676, Jun. 2002.

[14] A. D. Cheok and Y. Fukuda, "A new torque and flux control method for switched reluctance motor drive," IEEE Trans. Power Electron., vol. 17, no. 4, pp. 543-557, Jul. 2002.

[15] Y. Zheng, H. Sun, Y. Dong, and W. Wang, "Torque ripple minimization with current oriented method for switched reluctance motor," in Proc. IEEE Intl. Conf. Elect. Mach. Syst., South Korea, pp. 1640-1644, Oct. 2007.

[16] N. Chayopitak, R. Pupadubsin, K. Tungpimolrut, P. Somsiri, P. Jitkreeyan, and S. Kachapornkul, "A adaptive low-ripple torque control of switched reluctance motor for small electric vehicle," in Proc. Intl. Conf. Elect. Mach. Syst. (ICEMS2008), Wuhan, China, pp. 3327-3332, Oct. 2008.

[17] D.-H. Lee, J. Liang, Z.-G. Lee, and J.-W. Ahn, "A simple nonlinear logical torque sharing function for low-torque ripple SR drive," IEEE Trans. Ind. Electron., vol. 56, no. 8, pp. 3021-3028, Aug. 2009.

[18] X. D. Xue, K. W. E. Cheng, and S. L. Ho, "Optimization and evaluation of torque-sharing functions for torque ripple minimization in switched reluctance motor drives," IEEE Trans. Power Electron., vol. 24, no. 9, pp.2076-2090, Sept. 2009.

[19] B. Blanque and A. Doria-Cerezo, "Torque ripple minimization for a switched reluctance motor," in Proc. European Conf. Power Electron. Appl. (EPE2009), Barcelona, Spain, pp. 1-8, Sept. 2009.

[20] C. Pavlitov, H. Chen, Y. Gorbounov, T. Tashev, T. Georgiev, W. Xing, "Switched reluctance motor torque ripples reduction by the aid of adaptive reference model," in Proc. Intl. Sym. Power Electron. Elect. Drives Automation Motion (SPEEDAM2010), Pisa, Italy, pp. 1276-1279, Jun. 2010.

[21] V. P. Vujicic, "Minimization of torque ripple and copper losses in switched reluctance drive," IEEE Trans. Power Electron., vol. 27, no. 1, pp. 388-399, Jan. 2011.

[22] M. M. Namazi, S. M. Saghaian-Nejad, A. Rashidi, and H. A. Zarchi, "Passivity-based adaptive sliding mode speed control of switched reluctance motor drive considering torque ripple reduction," in Proc. IEEE Intl. Elect. Mach. Drives Conf. (IEMDC2011), Niagara Falls, ON, USA, pp. 1480-1485, May 2011.

[23] J. Fort, B. Skala, and V. Kus, "The torque ripple reduction at the drive with the switched reluctance motor," in Proc. IEEE Intl. Power Electron. Motion Ctrl. Conf. (EPE-PEMC2012), Novi Sad, Servia, DS2a.16-1-4, Sept. 2012.

[24] R. Mitra and Y. Sozer, "Torque ripple minimization of switched reluctance motors through speed signal processing," in Proc. IEEE Energy Conversion Congr. Expo., Pittsburgh, PA,USA, pp. 1366-1373, Sept. 2014.

[25] W. Yi, Q. Ma, and J. Hu, "Torque ripple minimization of switched reluctance motors by controlling the phase currents during commutation," in Proc. Intl. Conf. Elect. Mach. Syst. (ICEMS2014), Hangzhou, China, pp. 1866-1870, Oct. 2014.

[26] J. Ye, B. Bilgin, and A. Emadi, "An extended-speed low-ripple torque control of switched reluctance motor drives," IEEE Trans. Power Electron., vol. 30, no. 3, pp. 1457-1470, Mar. 2015.

[27] H. Makino, S. Nagata, T. Kosaka, and N. Matsui, "Instantaneous current profiling control for minimizing torque ripple in switched reluctance servo motor," in Proc. IEEE Energy Conversion Congr. Expo., Montreal, QC, Canada, pp. 3941-3948, Sept. 2015.

[28] F. Yi and W. Cai, "Repetitive control-based current ripple reduction method with a multi-port power converter for SRM drive," in Proc. IEEE Transportation Electrification Conf. Expo., Dearborn, MI, USA, pp. 1-6, Jun. 2015.

[29] L. Du, B. Gu, J. S. Lai, and E. Swint, "Control of pseudo-sinusoidal switched reluctance motor with zero torque ripple and reduced input current ripple," in Proc. IEEE Energy Conversion Congr. Expo., Denver, CO, USA, pp. 3770-3775, Sept. 2013.

[30] E. Swint and J. Lai, "Switched reluctance motor without torque ripple or electrolytic capacitors," in Proc. IEEE Energy Conversion Congr. Expo., Phoenix, AZ, USA, pp. 1657-1663, Sept. 2011..